ELSEVIER

Chemical Geology 238 (2007) 72–83

CHEMICAL GEOLOGY
INCLUDING
ISOTOPE GEOSCIENCE

www.elsevier.com/locate/chemgeo

Rayleigh fractionation of iron isotopes during pedogenesis along a climate sequence of Hawaiian basalt

Aaron Thompson [a], Joaquin Ruiz [b], Oliver A. Chadwick [c], Monica Titus [a], Jon Chorover [a,*]

[a] *Department of Soil, Water and Environmental Science, University of Arizona, Tucson, AZ 85721, United States*
[b] *Department of Geosciences, University of Arizona, Tucson, AZ 85721, United States*
[c] *Department of Geography, University of California-Santa Barbara, CA 93106, United States*

Received 13 April 2006; received in revised form 31 October 2006; accepted 2 November 2006

Editor: C. Gopel

Abstract

We measured iron isotopic composition of surface (10–20 cm) and subsurface (50–70 cm) basaltic soil horizons from the Island of Maui along a climate gradient (MCG) ranging from 2.2 to 4.2 m mean annual precipitation (MAP). All soil forming factors except climate were conserved. The MCG has a documented decrease in Fe with increasing rainfall that is highly correlated with decreasing mean annual Eh values. We found that increasing MAP from 2.8 to 4.2 m resulted in a surface plus subsurface average increase of 0.56‰±0.09‰ δ^{56}Fe with the subsurface consistently 0.33±0.06‰ δ^{56}Fe greater than the surface horizons. Based on loss of Fe relative to Nb, Rayleigh fractionation was observed with $10^3 \ln\alpha_{lost-retained}$ values of −0.37±0.03 and −0.34±0.04 for the surface and subsurface, respectively. Equivalent $10^3 \ln\alpha_{lost-retained}$ values for the surface and subsurface soils suggests Fe loss is driven by similar mechanisms throughout the soil profile. Our calculated fractionation factor is about 1/3 the magnitude of laboratory determined fractionation factors for Fe reduction, suggesting other processes (organic complexation, Fe re-precipitation) modulate the net Fe loss along the MCG. These results offer field-scale confirmation of laboratory experiments on model systems that show anoxic weathering reactions produce materials enriched in heavy Fe isotopes.

Keywords: Fe isotopes; Soil; Redox; Pedogenesis

1. Introduction

The weathering reactions of iron (Fe) intersect with many aspects of the biogeochemical functioning of soils (Crews et al., 1995; Torn et al., 1997; Darke and Walbridge, 2000; Miller et al., 2001; Küsel et al., 2002). Thermodynamic transformation of initially ferrous-bearing primary basalt minerals in oxic environments is thought to involve rapid Fe oxidation to secondary short-range-ordered minerals like ferrihydrite or nano-goethite followed by slow transformation to crystalline Fe-oxides such as goethite [α-FeO(OH)] and hematite [α-Fe_2O_3] (Shoji et al., 1993). Conservation of Fe relative to Si and non-hydrolyzing cations (i.e., Na, Ca, etc.) is predicted based on the low aqueous solubility of Fe^{III}-solids, although some mobilization of Fe does occur via proton-promoted dissolution at pH < pznpc (point of zero net proton charge)

* Corresponding author.
E-mail address: Chorover@cals.arizona.edu (J. Chorover).

0009-2541/$ - see front matter © 2006 Elsevier B.V. All rights reserved.
doi:10.1016/j.chemgeo.2006.11.005

and to a greater extent via ligand-promoted dissolution when strong binding organic acids are present (Stewart et al., 2001; Chadwick et al., 2003; Jansen et al., 2003). Under conditions of oxygen limitation, Fe^{III} provides a terminal electron acceptor for anaerobic respiration (Lovley and Phillips, 1986) and complete loss of Fe from the soil profile is predicted to follow its reduction to the highly soluble Fe^{II} form. Thus, the three principal mechanisms for Fe removal from soil solids involve (1) proton-promoted dissolution, (2) complexation by organic ligands (e.g., ligand-promoted dissolution) under oxic conditions, and (3) reductive dissolution under anoxic conditions. Of these mechanisms, reductive dissolution is the most kinetically favorable (Cornell and Schwertmann, 1996) producing large Fe depletions when soils become anoxic (Ponnamperuma, 1972).

Until recently, evaluation of Fe weathering and transformation reactions has been limited to inferences from mass abundance measurements in the field (Wada and Wada, 1976; Parfitt et al., 1988) or carefully controlled simulations of weathering in the laboratory (Casey et al., 1993; Hinsinger et al., 2001; White and Brantley, 2003). Analytical advances in multi-collector ICP-MS technology provide the potential of additional information from the four naturally occurring isotopes of Fe: ^{54}Fe, ^{56}Fe, ^{57}Fe and ^{58}Fe. Although Fe isotopic systems are among the most analytically challenging (Arnold et al., 2004), their potential contribution to our understanding of soil formation is considerable. Fe is the fourth most abundant element in the earth's crust, a major player in weathering systems and a dominant regulator of soil solution chemistry (Schwertmann, 1991). Fe isotopes may provide information on the processes and sources controlling pedogenesis of Fe-bearing minerals in field settings.

Previous laboratory and theoretical work indicates that both ligand-promoted (Brantley et al., 2001; Brantley et al., 2004) and reductive (Beard et al., 1999; Beard et al., 2003) dissolution of Fe minerals results in preferential removal of the lighter isotope (Johnson et al., 2004), thereby enriching the residual solids in the heavier isotope. Conversely, proton-promoted dissolution results in no detectable isotopic fractionation (Skulan et al., 2002; Wiederhold et al., 2006). Furthermore, adsorption processes are known to preferentially sequester the heavier isotope at soil particle surfaces (Icopini et al., 2004) and precipitation of ferric oxides from Fe^{II}(aq) also yields isotopically heavy solid phases (Bullen et al., 2001; Balci et al., 2006). Consistent with these experimental data, Fantle and DePaolo (2004) found that dilute rivers in the western U.S. are generally enriched in light Fe isotopes, although river colloidal material has variable isotopic composition and can become enriched in heavy Fe isotopes during high sediment loads (Ingri et al., 2006). Thus, we predict that heavy isotope enrichment in the solid-phase should increase over the course of soil weathering, particularly in cases where reductive or ligand-promoted dissolution predominate.

To date, only a few Fe isotopes measurements on soils have been published, including: depth profiles of a semi-arid Inceptisol from Israel and a Spodosol from the Czech Republic (Emmanuel et al., 2005), a depth profile of a Costal Californian Ultisol (Fantle and DePaolo, 2004) and the B-horizon of a New York forest soil (Brantley et al., 2001). Soil-forming factors were not sufficiently controlled or characterized in these studies to allow us to evaluate the influence of weathering on Fe isotopic composition. So we sought to test our hypothesis by focusing on pedogenic Fe loss via reductive (and possibly ligand-promoted) dissolution using a set of soils formed within an established climate gradient in Hawaiian basalt (Chadwick and Chorover, 2001; Miller et al., 2001; Schuur and Matson, 2001; Chadwick et al., 2003). The use of pedogenic gradients is particularly advantageous for examining complex, temporally and spatially variable processes such as Fe dissolution and precipitation. Isolating a systematic increase in one soil-forming factor along a gradient allows trends and threshold behavior to be distinguished from the inherent variability of heterogeneous soil systems. The Hawaiian islands are especially well-suited for studying pedogenesis because the principal soil-forming factors (Jenny, 1941) can be controlled by careful site selection. In this work, surface and subsurface soils were collected from the Maui climate gradient (MCG) (Miller et al., 2001; Schuur and Matson, 2001; Scribner et al., 2006) to evaluate the effects of field redox conditions on Fe isotope fractionation. In addition to measuring Fe isotopes on whole soils, we made isotopic measurements on chemical extractions targeting: (i) the most readily soluble and adsorbed forms of Fe and (ii) Fe associated with organic matter. We hypothesized that whole soil $\delta^{56}Fe$ values would be directly related to weathering intensity. Our data support this hypothesis for soil systems where reductive dissolution appears to be the principal mechanism of Fe removal.

2. Materials and methods

2.1. Site selection

The Hawaiian islands are well suited for studying pedogenic processes because the five state factors

controlling pedogenesis (Jenny, 1941) are either tightly constrained (parent material and vegetation composition) or vary systematically (slope, soil age and local climate) across the archipelago. For this study, we collected soils from an established and well-characterized gradient in mean annual precipitation [the Maui Climate Gradient (MCG)], along a single-aged lava flow, in which all factors except rainfall are conserved (Miller et al., 2001; Schuur and Matson, 2001). All soils were formed from basaltic parent materials (Vitousek, 2004), all sites are located in montane rainforest dominated by the tree species *Meterosideros polymorpha* on level terrain at 1130 to 1500 m elevation, with mean annual soil temperature of 16 °C and a substrate age of 410 ka (Schuur and Matson, 2001). Prior work along the MCG has documented a correlation between pedogenic Fe and mean annual Eh (Fig. 1) (Chadwick and Chorover, 2001). This correlation strongly suggests reductive dissolution controls Fe loss along the MCG (likely outweighing other mechanisms such as proton or ligand-promoted dissolution) and thus provides an ideal location for testing our hypothesis regarding Fe isotope fractionation during weathering. The Fe mineral composition of the MCG soils consists largely of short-range-ordered (SRO) minerals and organically complexed Fe that are characteristic of the intermediate (410 ka) weathering stage in basalt-derived soils subjected to a humid climate (Chorover et al., 2004). XRD measurements of these soils typically reveal some crystalline goethite and/or hematite and small quantities of muscovite and kaolinite, but the bulk of the signal comes from XRD-amorphous material (Thompson et al., 2006b). ^{57}Fe Mössbauer of the Ag horizon at the 3500-mm site indicates nano (SRO)- and microcrystalline goethite accounts for ~75% of spectral area (Thompson et al., 2006b). A full Mössbauer study of all the MCG soils is currently underway.

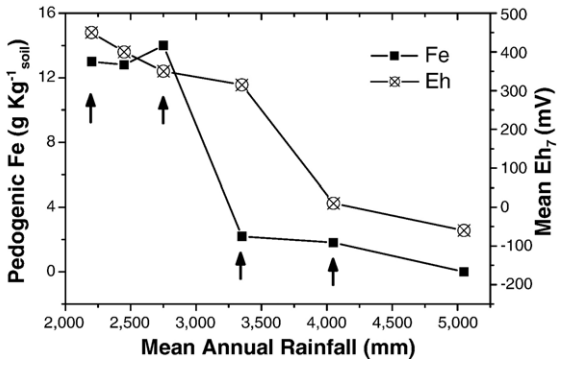

Fig. 1. Correlation of long-term average redox potential (360 platinum electrode measurements taken every 6 weeks over 18 months) with whole profile weighted averages of pedogenic Fe (sum of sequential Na–pyrophosphate, oxalate and dithionite-citrate extracts) across the MCG. Note all Eh measurements were adjusted to pH 7 assuming $Eh_7 = E_{pH°} - 59(7 - pH°)$, where $E_{pH°}$ and pH° are the measured soil Eh (mV) and pH, respectively. Data taken from Chadwick and Chorover (2001), Miller et al. (2001) and Schuur and Matson (2001). The arrows indicate sites sampled for this Fe isotope study.

2.2. Soil collection

The soils were collected by genetic horizon from pit faces (see Table 1 for horizon designations) excavated to greater than 1 m depth or to rock at four sites ranging in mean annual precipitation (MAP) from 2200 to 4200 mm. Taxonomic classification of the soils is as follows (site rainfall in parentheses): (1) Andic Dystrudept (2200 mm MAP); (2) Andic Dystrudept (2800 mm MAP); (3) Acrudoxic Hydrudand (3500 mm MAP); and (4) Aquandic Epiaquept (4200 mm MAP). Soils from the drier two sites (2200 and 2800 mm MAP) were double-bagged in 1.75 mil polyethylene bags with moist paper towels between the layers and placed immediately on ice, according to procedures described in Bartlett and James (1993). For the wetter two sites (3500 and 4200 mm MAP), soil horizons were classified as either oxic or anoxic based on the presence/absence of redoximorphic features (mottles, standing water, hydrogen sulfide odor, etc.). Samples considered oxic were treated similarly to soils from the drier sites; anoxic soils were collected as outlined in Thompson et al. (2006b). All soils were then packed on blue ice in coolers for transport to the lab where the majority of each soil horizon was homogenized and stored at 4 °C. All handling of the anoxic soils was done in a 95% N_2, 5% H_2 glovebox.

2.3. Soil characterization

A standard chemical characterization of all soils was conducted. Total element concentrations were measured following Li-metaborate fusion (Hossner, 1996), and "labile" element concentrations were measured using 0.5 M HCl (Lovley and Phillips, 1986), 0.1 M acid ammonium oxalate (AAO) or Na–pyrophosphate extractions (Loeppert and Inskeep, 1996). The HCl and AAO extractions were selected to target the short-range-ordered iron (SRO-Fe) component of the soil that likely represents the most readably soluble Fe. In previous work, we have observed good correlation between AAO extractable Fe and an SRO-Fe component with a magnetic ordering temperature near 4K best identified as "nano-goethite" by Mössbauer spectroscopy (Thompson et al., 2006b). The Na–pyrophosphate

Table 1
Fe mass concentrations (g kg^{-1})

Horizon	Total [a]	τ_{Fe}	HCl	Na–Pyro	Oxalate
Surface (10–20 cm)					
2200 mm (A) [b]	283.0 (198)	−0.36	24.8 (14)	108.9 (83)	59.0 (34)
2800 mm (A)	156.0 (109)	−0.39	16.0 (46)	64.2 (16)	38.6 (5)
3500 mm (Ag)	97.0 (68)	−0.79	27.7 (16)	33.8 (26)	41.5 (25)
4200 mm (A)	6.2 (4)	−0.87	1.8 (1)	3.9 (2)	5.3 (4)
Subsurface (50–70 cm)					
2200 mm (Bw3)	129.4 (91)	−0.14	17.0 (26)	46.8 (5)	38.4 (5)
2800 mm (Bw3)	165.1 (116)	−0.47	5.0 (5)	75.9 (41)	42.4 (72)
3500 mm (Bw4)	54.3 (38)	−0.71	1.6 (1)	11.3 (10)	10.0 (14)
4200 mm (Bg3)	27.3 (19)	−0.89	0.5 (0)	2.6 (12)	2.1 (0)
Depth profile (3500 mm MAP)					
6–13 cm (Ag)	97.0 (68)	−0.79	27.7 (16)	33.8 (26)	41.5 (25)
13–23 cm (Bw1)	76.0 (53)	−0.82	8.3 (13)	41.8 (18)	34.5 (13)
40–58 cm (Bw3)	54.3 (38)	−0.71	1.6 (1)	11.3 (10)	10.0 (14)
58–85 cm (Bw4)	66.5 (47)	−0.70	1.6 (0)	3.0 (8)	6.0 (10)

[a] Errors are 1 standard deviation (1σ) based on three replicate samples except for total Fe, which are based on triplicate analysis of a single sample. Uncertainty is presented as the error in the last digit in concise notation (e.g., 5.0(15)=5.0±1.5).
[b] Soil horizon designations are those assigned in the field by inspection during sampling.

extraction targets organic-bound Fe and Fe that is occluded within organic colloids that are dispersed in the high pH of this solution. All extractions were performed at a 1:60 solid to solution mass ratio in 50 mL PPCO centrifuge tubes for 2 h. Tubes were centrifuged for 20 min at 41,500 relative centrifugal force and supernatant solutions were then analyzed using inductively coupled plasma-mass spectrometry (Perkin Elmer DRC II ICP-MS).

Total soil digestions for Fe isotope analysis were first ashed at 550 °C in an air atmosphere for 3 h to remove organic matter. Then, 600 mg of the residue was mixed at a ratio of 1:5 with ultrapure (99.999%) $LiBO_2$ flux (Spex Certiprep: certified 7 mg kg^{-1} Fe) and fused at 1100 °C for 15 min in ultrapure graphite crucibles (Spec Certiprep). After fusion, the samples were dissolved in 2 M HNO_3 (Optima: Fisher Scientific) and analyzed via ICP-MS for Fe concentration. Aliquots of these digestions and the above HCl and Na–pyrophosphate extractions were purified for Fe isotope analysis as outlined below.

2.4. Fe purification

Fe purification of the samples was accomplished following the procedure outlined in Skulan et al. (2002) using a total of 75 μg of Fe per sample applied to an anion exchange resin. Prior to purification, we cleaned the anion exchange resin (Bio-Rad AG 1X3 200-400 mesh) by packing it in a 250-ml glass column and backflushing (against gravity) with acids and water as follows: 500 ml of 2% HNO_3 (Omnitrace: Fisher Scientific) was pumped through the resin, followed by 250 ml of 18 MΩ H_2O. This sequence was repeated three times and then followed by 250 ml of Baseline (Seastar) 0.5 M HCl, which was the resin storage matrix. The elution from each round of rinsing was analyzed for Fe and Ca (the latter because of potential isobaric interference) by ICP-MS. Fe and Ca values in the samples were identical within error to the blanks after the first pass of HNO_3–H_2O.

To purify the whole soil digests and selective extraction solutions, aliquots of each solution containing 75 μg of Fe were brought to dryness in a Teflon bomb (Savallex), 1 ml of concentrated HNO_3 and 30 μl of H_2O_2 (Optima: Fisher Scientific) were added, and then the bomb was sealed and digested for 10 min with periodic venting to destroy any organic material. The solution was brought again to dryness. Two milliliters of 7 M HCl (Baseline: Seastar) was added and an aliquot (100 μl) was taken to allow calculation of Fe recovery. Samples were added to a pre-cleaned anion resin (Bio-Rad AG 1X3 200-400 mesh) contained in a polypropylene column (Bio-Rad #731-1550) rinsed 3× with 9 ml of 7 M HCl and then eluted with 4× rinses of 1.5 ml of 0.5 M HCl. The resulting elution was evaporated to dryness, resuspended in 2 ml of 7 M HCl and the process was repeated in a second resin column. This second elution was evaporated to dryness and resuspended in 0.05 M or 0.1 M HNO_3. An aliquot of this resuspension was analyzed for total Fe and Ca concentration and then

diluted appropriately for multicollector analysis. We checked recovery of the Fe purification procedure by measuring aliquots before and after each ion-exchange resin pass. Only those purifications indicating complete (within error) recovery of applied Fe were included in multi-collector analysis.

2.5. Fe isotope measurement

Samples were introduced using a low-flow (100 μl min^{-1}) desolvating nebulizer (Aridus by Cetac) at a concentration between 2 and 5 mg kg^{-1} Fe in order to produce a 3×10^{-10} A ^{56}Fe signal (system sensitivity improved after several instrument upgrades). All masses except ^{56}Fe were measured on Faraday collectors using 10^{11} Ω resistors; ^{56}Fe was measured using a 10^{10}-Ω resistor. The *Isoprobe* was operated in "soft extraction" mode, which reduces instrument signal intensity, but significantly improves signal to noise relative to "hard extraction" mode. Iron isotope measurements were made by simultaneous collection of ^{54}Fe, ^{56}Fe, ^{57}Fe. ^{52}Cr was monitored for isobaric interference of ^{54}Cr on ^{54}Fe; however, no chromium correction was applied to the ^{54}Fe signal as variability on the low intensity mass 52 signal was quite high, likely representing system noise, and it never contributed more than 0.006‰ to $\delta^{56}Fe$ values. Mass-bias corrections were accomplished using a standard-sample-standard bracketing approach (Albarede and Beard, 2004), with isotopic compositions measured relative to the IRMM-014 Fe isotope standard (Taylor et al., 1992). Throughout an analytical session, IRMM standards of varying Fe concentration (e.g., 2.5, 5 and 7.5 mg kg^{-1} when samples were introduced at 5 mg kg^{-1}) were measured as samples to determine Fe concentration-dependent mass bias (Mullane et al., 2002; Albarede and Beard, 2004). For each analytical session, we linearly regressed $\delta^{56}Fe$ against the ^{56}Fe voltage reading for these concentration standards and used this regression to correct the Fe isotopic composition of all samples for small deviations from the target Fe concentration (e.g., 5 mg kg^{-1}). Typically, ^{56}Fe intensity varied less than 10% between samples and bracket standards, so in most cases this correction amounted to less than 0.1‰. Nonetheless, it greatly improved precision between replicates.

2.6. Fe isotope reporting and method considerations

Isotopic compositions are reported using standard delta notation in units of per mil (parts per 1000 or ‰):

$$\delta^{56}Fe = [(R_{sample}/R_{IRMM-014}) - 1]\cdot10^{3}, \quad (1)$$

where $R = {}^{56}Fe/{}^{54}Fe$ and $R_{IRMM\text{-}014}$ is the ratio of the IRMM metal standard (Taylor et al., 1992). The average-earth $\delta^{56}Fe$ value proposed by Beard et al. (2003) is $+0.09\pm0.05$‰ (1 SD) on this scale. All soil sample data plot along the theoretical $\delta^{57}Fe = 1.5\cdot\delta^{56}Fe$ line (Fig. 2) indicating that isobaric interferences did not significantly affect our analysis and thus only $\delta^{56}Fe$ values are reported.

For total soil digests, we purified Fe from $LiBO_2$ fusions that had some background Fe contamination from the ultrapure (99.999%) $LiBO_2$ flux (Spex Certiprep: certified 7 mg kg^{-1} Fe). To assess the impact of this contamination, we combined blanks from many fusions to obtain enough Fe for isotopic measurement (albeit at a lower than ideal concentration) and determined a $\delta^{56}Fe$ mean±two standard deviation (2SD) value of $+3.6\pm0.8$‰$_{IRMM\text{-}014}$ for the purified $LiBO_2$ blank. Next, we compared Fe sample–blank ratios for each of the soils; the soil with the lowest organic-free Fe content (Surface, 4200 mm MAP) had an Fe sample–blank ratio of ~370. This amounted to a maximum 0.01‰ error in the $\delta^{56}Fe$ average for the Maui 4200 MAP sample (+0.39‰$_{IRMM\text{-}014}$). All other samples had greater Fe sample–blank ratios, many by 1–2 orders of magnitude, and thus all values were reported as measured.

Prior work on a similar GVI *Isoprobe* indicated the possibility of significant interference of ^{57}Fe by CaOH isobars (Beard et al., 2003). We examined this possibility by preparing mixtures of Fe and Ca ICP-standards from Fe/Ca=100,000 (g Fe/g Ca) to Fe/Ca=100. All values plotted along the theoretical $\delta^{57}Fe = 1.5\cdot\delta^{56}Fe$ line indicating CaOH interference was minimal (Fig. 3), although a slight increase in both $\delta^{56}Fe$ and $\delta^{57}Fe$ with

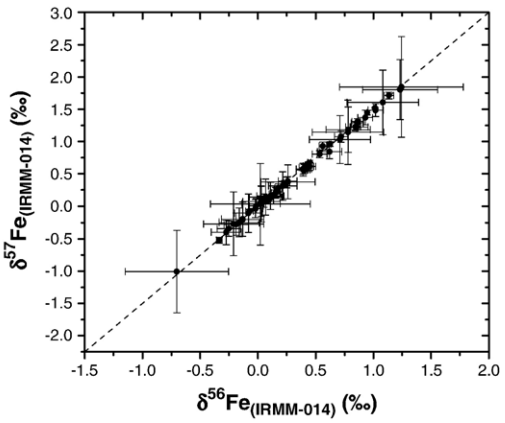

Fig. 2. $\delta^{56}Fe$ vs. $\delta^{57}Fe$ for all soil samples measured. The diagonal line indicates the theoretical mass-dependent fractionation between $\delta^{56}Fe$ and $\delta^{57}Fe$. Error bars are 2σ based on two to four replicates.

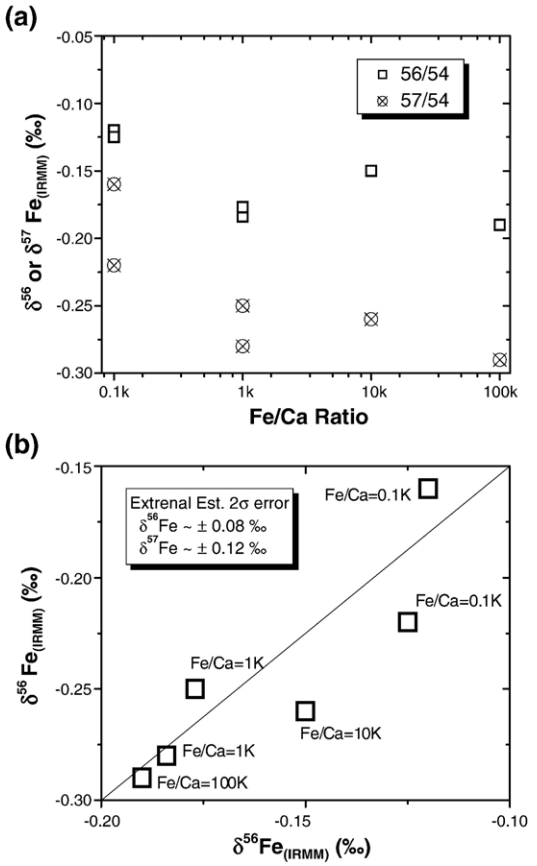

Fig. 3. δ^{56}Fe and δ^{57}Fe for mixtures of plasma grade ICP standards (isotopic ratio previously unmeasured) plotted against (a) Fe/Ca ratio and (b) on a δ–δ plot. The diagonal line indicates the theoretical mass dependent fractionation between δ^{56}Fe and δ^{57}Fe. Note, each point represents a single measurement carried out to test the influence of Ca of Fe isotopic measurements. 2σ errors estimated from 5 replicate measurements of the IRMM-014 standard are shown in part (b). All data points are equal within these estimated 2σ error limits.

decreasing Fe/Ca might indicate a matrix effect as described by Arnold et al. (2004). Fe/Ca ratios on all measured soil samples were in the 1000 to 10,000 range after two passes through ion exchange columns. An instrument upgrade just prior to the start of our measurements allowed us to operate the *Isoprobe* in "soft extraction" mode (rather than the default "hard extraction" mode) and this likely explains the discrepancy between our results and prior measurements (Beard et al., 2003).

2.7. Calculations and notation

Loss and gain of Fe was computed by applying a simplified version of the open-chemical-system transport function (Chadwick et al., 1990), which ignores physical collapse and dilation of the soil column. The mass fraction of Fe lost (or gained) from a soil horizon relative to the mass of Fe originally present in the parent material is calculated from the equation (Kurtz et al., 2000):

$$\tau_{\mathrm{Fe},w} = \left(\frac{C_{\mathrm{Fe},w}}{C_{\mathrm{Fe},p}} \times \frac{C_{i,w}}{C_{i,p}}\right) - 1, \quad (2)$$

where C is the concentration of an element in g kg^{-1}, the subscript w refers to the weathered material, the subscript p refers to the parent material and subscript i refers to the least mobile element. For the Hawaiian islands, Nb has been determined to be the least mobile element (Kurtz et al., 2000; Scribner et al., 2006). Negative values of $\tau_{Fe,w}$ indicate loss of Fe from that soil horizon, while positive values indicate enrichment.

Portions of the Fe isotope composition data set were fit to a Rayleigh fractionation model using the formula:

$$\delta^{56}\mathrm{Fe}_w \approx (\delta^{56}\mathrm{Fe}_o + 10^3) f^{\alpha_{lost-retained}-1} - 10^3, \quad (3)$$

where $\delta^{56}\mathrm{Fe}_o$ is the isotopic composition of the starting material, $f = \tau_{\mathrm{Fe,w}} + 1$ and $\alpha_{\text{lost-retained}}$ describes the fractionation between Fe lost and that retained in the soil. This arrangement ($\alpha_{\text{soln-solid}}$) was adopted to maintain consistency with notation used elsewhere to describe fractionation between aqueous and solid Fe species (Skulan et al., 2002; Beard et al., 2003; Brantley et al., 2004; Anbar et al., 2005). In our application, we allow $\delta^{56}\mathrm{Fe}_o$ to deviate from the reported isotopic composition of the basaltic parent material in Hawaii [$\delta^{56}\mathrm{Fe}_{\text{IRMM-014}} = -0.10 \pm 0.03$‰ (1SD) from Beard et al. (2003)], which included both theolitic and alkalic basalts.

Errors on isotopic measurements are reported as external 2σ errors based on multiple analysis of the samples (typically three replicates), whereas errors on chemical values are given as 1σ errors (1SD). Regression statistics were determined using Origin graphical analysis software (OriginLab Corp.) and are presented as 1 standard error (1SE). Errors were propagated using standard deviations following standard methods of error propagation in arithmetic calculations (Skoog et al., 1997) and then converted to 2σ errors. Throughout the text, the errors are presented as the error in the last digit using concise notation (e.g., 5.0(15) = 5.0 ± 1.5).

3. Results

3.1. Non-isotopic soil characterization

Total Fe and Fe solubilized by 0.5 M HCl (HCl), acidic ammonium oxalate (AAO) and Na–pyrophosphate (Na–

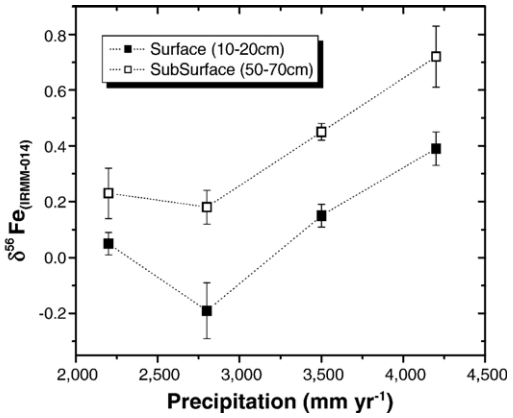

Fig. 4. δ^{56}Fe values for a surface and subsurface transect along the climate gradient (MCG). Error bars are 2σ based on two to four replicates.

Pyro) are listed in Table 1. The MCG sequence exhibits a systematic decrease in total Fe with increasing rainfall (Fig. 1). This has been correlated with a decrease in mean annual Eh (measured weekly) and signifies an increasing prevalence of anoxic conditions at the higher rainfall sites (Miller et al., 2001; Schuur and Matson, 2001). Na–Pyro, AAO and HCl extractable Fe all increase as a fraction of total Fe with increasing rainfall (Table 1). τ_{Fe} values systematically decrease with increasing rainfall reaching ca. −0.9 at the highest rainfall site (Table 1).

3.2. MCG Fe isotopic compositions

Fe isotope ratios of whole soil digests from the MCG increase systematically with rainfall in both the surface and subsurface horizons (Fig. 4). The δ^{56}Fe values also increase with depth, as illustrated by the four horizons selected from the 3500-mm MAP site (Fig. 5). Omitting the 2200-mm

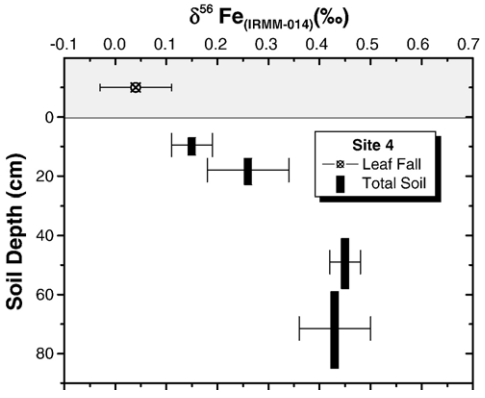

Fig. 5. Measured δ^{56}Fe values for a depth profile at the 3500-mm MAP site and associated leaf-fall. Error bars are 2σ based on two to four replicates. The black bars denote the thickness of soil homogenized for each measurement.

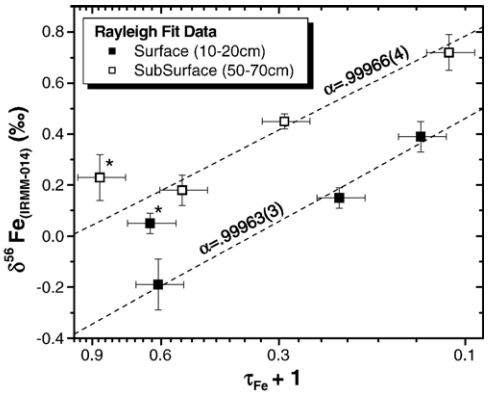

Fig. 6. Measured δ^{56}Fe values for transects along the climate gradient (MCG) as a function of the fraction of Fe remaining (τ+1). Dashed lines indicate Rayleigh fractionation fits with α shown calculated by excluding the 2200-mm MAP site (*). Error bars are 2σ based on two to four replicates.

MAP site, δ^{56}Fe values for the remaining three sites fall along a Rayleigh fractionation line with α values for the surface and subsurface horizons of 0.99963(3) and 0.99966(4) (1SE), respectively (Fig. 6). This translates into $10^3 \ln\alpha_{lost-retained}$ values of −0.37(3) and −0.34(4) for the surface and subsurface horizons, respectively.

We assessed differences between the isotopic composition of the "labile" (HCl or Na–pyro extracted) and residual soil Fe pools by comparing $\delta^{56}Fe_{HCl}$ and $\delta^{56}Fe_{Pyro}$ to the calculated residual soil δ^{56}Fe after extraction using the formula:

$$\Delta_{Ext-Res}(‰) = \delta^{56}Fe_{Ext} - \frac{\delta^{56}Fe_{Tot} - (\delta^{56}Fe_{Ext})(f_{Ext})}{1 - f_{Ext}}, \quad (4)$$

where the subscript "Ext" refers to either the HCl or the Na–pyrophosphate extract, the subscript "Tot" refers to total soil digest and f_{Ext} is the fractional recovery of total Fe by the extract. This presentation illustrates the isotopic gap between Fe in the "labile" and residual pools. The two labile Fe pools we sampled (HCl extractable Fe-oxides and organic-bound Fe) generally tracked the total soil isotopic composition (Table 2) with $\Delta_{Ext-Res}$ values varying minimally with increasing rainfall (Fig. 7). The exception is for the labile Fe-oxides in the subsurface soils. Here, $\Delta_{HCl-Res}$ values are consistently greater than +0.3‰, with a peak of +0.70(8)‰ at the 2800-mm MAP site.

4. Discussion

4.1. General system behavior

The sequence of soils studied here represents an end-member weathering scenario where leaching rates are

high and dissolution products generally do not accumulate but are either translocated to lower horizons or completely removed from the soil profile. In this weathering scenario, Fe is expected to persist relative to Si and the base cations unless it is strongly complexed by soluble organics (such as occurs in a podzol) or anoxic conditions arise. In the MCG, loss of Fe (denoted by negative values of τ_{Fe} in Table 1) is directly correlated to increases in rainfall above 2800 mm MAP. A corresponding inverse relationship with between mean annual Eh and rainfall (Fig. 1) strongly suggests Fe loss is triggered by anoxic conditions. However, we cannot rule out contributions from organic-ligand promoted dissolution. These soils contain considerable quantities of organic matter (80 to 500 g C kg^{-1} dry soil), high DOC values (~100 mg C L^{-1}) and large portions of the soil Fe mass can be extracted by Na–pyrophosphate (Table 1). This implies organic complexation of Fe is extensive and, given the low pH of these soils (generally less than 4.5), suggests organic-ligand promoted dissolution and mobilization of Fe occurs throughout the gradient. Nonetheless, the MGC is well constrained in terms of pedogenic influences such that controlled variation in precipitation—which again has been shown to correlate indirectly with mean annual Eh (Schuur and Matson, 2001)—is the only independent variable. Thus, we believe that while organic complexation does drive dissolution in these soils, its contribution is more uniform across all sites than reductive dissolution, which can be expected to increase significantly as soil pores become water-filled for progressively longer periods of time in response to greater precipitation. We can similarly dismiss contributions from proton-promoted dissolution by noting that soil pH is not correlated with rainfall (Schuur and Matson, 2001); again, proton-promoted dissolution may contribute to overall Fe loss, but we expect that contribution to be similar at all sites. Thus, by examining the response of these soils to variation in rainfall we can reasonably isolate the pedogenic response to reductive Fe dissolution.

4.2. Rayleigh fractionation along the MCG

We have adopted the use of a Rayleigh fractionation model assuming the whole soil Fe pool is equally "active" over the course of soil development. We recognize that Fe dissolution processes involve only a small "weathering front" (Wiederhold et al., 2006), but there is good evidence for extensive re-cycling of Fe within the soil profile—for instance primary Fe bearing minerals are difficult to detect by ^{57}Fe Mössbauer after even 20 ka of weathering at 2500 mm MAP (Thompson, unpublished data)—such that the full pool of soil Fe can be assumed to have participated in dissolution–precipitation events.

Fe isotope data from the MCG provide strong support for our hypothesis that solid-phase δ^{56}Fe values are

Table 2
Fe isotopic compositions ($\delta^{56}Fe_{IRMM\text{-}014}$)

Horizon	Total	HCl	Na–Pyro	HCl-residual [a]	Pyro-residual [a]
Surface A horizons (10–20 cm)					
2200 mm (A) [b]	0.05 (4) [c]	0.23 (6)	0.07 (2)	0.03 (5)	0.04 (4)
2800 mm (A)	−0.19 (10)	−0.34 (5)	−0.07 (7)	−0.17 (7)	−0.27 (7)
3500 mm (Ag)	0.15 (4)	0.02 (6)	0.16 (5)	0.20 (5)	0.14 (5)
4200 mm (A)	0.39 (6)	0.45 (10)	0.39 (12)	0.37 (9)	0.39 (8)
Subsurface Bw horizon (50–70 cm)					
2200 mm (Bw3)	0.23 (9)	0.56 (7)	0.24 (3)	0.18 (11)	0.22 (8)
2800 mm (Bw3)	0.18 (6)	0.86 (10)	0.41 (5)	0.16 (7)	−0.02 (7)
3500 mm (Bw4)	0.45 (3)	0.84 (9)	0.44 (8)	0.44 (4)	0.45 (6)
4200 mm (Bg3)	0.72 (11)	1.02 (13)	0.86 (10)	0.71 (11)	0.71 (21)
Depth profile (3500 mm site)					
6–13 cm (Ag)	0.15 (4)	0.02 (6)	0.16 (5)	0.20 (5)	0.14 (5)
13–23 cm (Bw1)	0.26 (8)	0.62 (2)	0.44 (6)	0.25 (11)	0.04 (7)
40–58 cm (Bw3)	0.45 (3)	0.84 (9)	0.44 (8)	0.44 (4)	0.45 (6)
58–85 cm (Bw4)	0.43 (7)	0.93 (13)	0.43 (3)	0.42 (8)	0.43 (8)

[a] These parameters are calculated as $\delta^{56}Fe_{residual}(‰) = \frac{\delta^{56}Fe_{Tot} - (\delta^{56}Fe_{Ext})(f_{Ext})}{1 - f_{Ext}}$ and represent the isotopic value of the un-extractable portion of the soil.

[b] Soil horizon designations are those assigned in the field by inspection during sampling.

[c] Uncertainties are 2*standard deviation (2σ) based on two to four replicate samples, presented as the error in the last digit in concise notation (e.g., 5.0(15)=5.0±1.5).

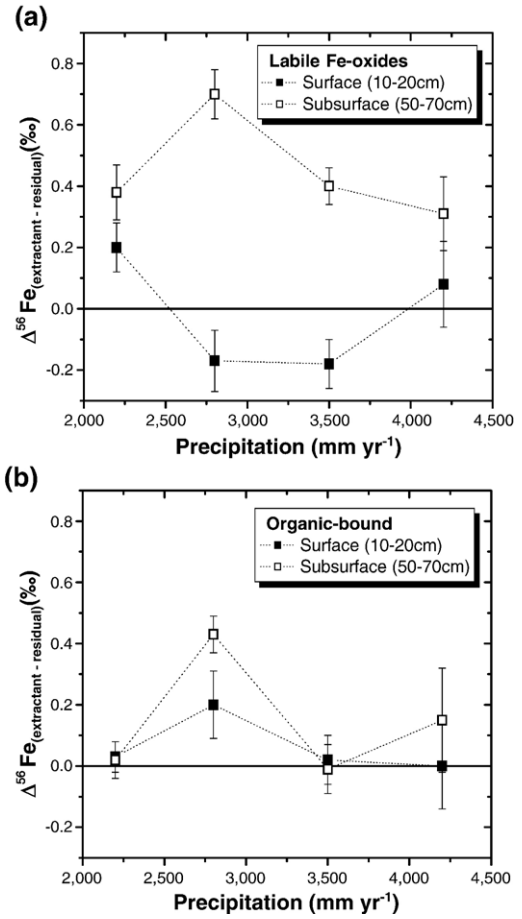

Fig. 7. Difference between measured δ^{56}Fe value in extractant and the residual soil calculated by mass balance for a 0.5-M HCl extraction (a) and a Na–pyrophosphate extraction (b) along the climate gradient. This presentation indicates the isotopic gap between the labile phases and the residual soil Fe. Error bars are 2σ based on two to four replicates.

directly related to weathering intensity. The tight fit and consistent slope of the Rayleigh fractionation lines for both the surface and subsurface horizons in the wettest three sites (Fig. 6) suggest that the mechanisms controlling Fe loss are similar throughout the soil profile and between 2800 mm MAP and 4200 mm MAP. We calculate that $10^3\ln\alpha_{lost-retained}$ values for the MCG_{Sur} and MCG_{SS} are equal within error at −0.37(3) and −0.34(4), respectively. These values are consistent in sign, but lower in magnitude than fractionation factors determined experimentally for reductive dissolution of ferrihydrite (Fh) ($10^3\ln\alpha_{Fe(II)-Fh} \approx -1.3$; Beard et al., 1999; Beard et al., 2003), goethite (Gt) ($10^3\ln\alpha_{Fe(II)-Gt} \approx -1.2$; Icopini et al., 2004) and hematite (Hm) ($10^3\ln\alpha_{Fe(II)-Hm} \approx -1.3$; Beard et al., 2003). These laboratory-determined fractionation factors also include fractionation due to the adsorption of Fe^{II} to ferric-oxide particle surfaces (Icopini et al., 2004), which is likely minimal at the low pH (<4.5, Schuur and Matson, 2001) of these soils (Jeon et al., 2001)—although adsorption to organic matter may be significant. However, in the laboratory experiments adsorptive fractionation accounts for only a minor portion (∼−0.25) of the isotopic fractionation factor (Icopini et al., 2004; Crosby et al., 2005). Thus, even when corrected for adsorption, laboratory-determined $10^3\ln\alpha_{Fe(II)-Fe\text{-}solid}$ values for Fe reduction (ca. ∼−1.0) are still three times the magnitude of those calculated for the MCG (ca. −0.36). Thus, there appears to be some mechanism that modulates the overall loss of light Fe due to reductive dissolution in open field systems—either facilitating partial retention of light Fe or partial loss of heavy Fe.

Many scenarios can be proposed to explain this observation. Organic complexation (Brantley et al., 2001; Matthews et al., 2001; Wiederhold et al., 2006), re-oxidation/precipitation (Bullen et al., 2001; Balci et al., 2006) and the development of isotopically distinct surface coatings (Severmann et al., 2006; Wiederhold et al., 2006) are all likely involved in modulating the degree of net isotopic fractionation during weathering. Field-based evidence for Fe re-precipitation can be found in the high variability of field Eh measurements (Schuur and Matson, 2001) and directly in the form of mottles that are present to some degree at all sites. Coupling this with high DOC concentrations suggestive of significant organic complexation leads one to acknowledge an internal complexity in Fe cycling that precludes accurate discrimination of individual fractionation processes at this time. However, this recognition does not diminish the key finding: the net result of open system Fe cycling (dissolution–complexation–precipitation) favors the removal of light Fe from the soil profile when total Fe loss is dominated by reductive dissolution.

4.3. Selective extractions

In contrast with our measurements, prior Fe isotopic studies have generally observed negative $\delta^{56}Fe_{IRMM\text{-}014}$ values for soils (Brantley et al., 2001; Fantle and DePaolo, 2004; Emmanuel et al., 2005), indicating either a net gain of light Fe or a net loss of heavy Fe (assuming an "average-earth" parent material; Beard et al., 2003). Unfortunately, these studies did not include data for an "immobile" element (i.e., Ti, Nb, etc.) that would allow us to construct a pedogenic Fe mass balance (e.g., τ_{Fe}). Furthermore, the heterogeneity of soils complicates interpretation of Fe pedogenic processing from single profile measurements unless those

processes are so dominant (e.g., Fe translocation in Spodosols) as to overprint the inherent variability. What is generally applicable from these prior studies are data from selective chemical extractions that describe distinct pools of both isotopically heavy and light Fe in soils (Brantley et al., 2001; Fantle and DePaolo, 2004; Emmanuel et al., 2005). Our selective extractions of the MCG soils echo this observation (Fig. 7), with perhaps a tendency towards heavy isotope enrichment in the dilute HCl (targeting labile Fe-oxides and adsorbed Fe^{II}) and pyrophosphate (targeting organic matter) extractions relative to the residual soil. Aside from this observation these labile Fe pools do not exhibit a discernable response to rainfall during pedogenesis. This is perhaps because these labile pools are more representative of a "snapshot" distribution characteristic of the sampling time rather than a long-term pedogenic response. In prior experimental work (Thompson et al., 2006b), we have observed large-scale fluctuations in the size and composition of 0.5 M HCl extracts in response to oscillations in Fe reducing and oxidizing conditions. Future experimental work is necessary to describe the isotopic composition of these labile soil pools in relation to Fe biogeochemical processes.

4.4. Isotopically light surface horizons

The application of Rayleigh modeling also allows a prediction of the isotopic composition of the parent material ($\tau_{Fe}=0$) with δ^{56}Fe values of −0.38(5)‰ and −0.01(7)‰ for the surface and subsurface soils, respectively. For the subsurface soil, this is equal within error to the average δ^{56}Fe of Hawaii basalts (−0.10 (3)‰; Beard et al., 2003) suggesting that reductive dissolution has acted consistently on unweathered basalt at depth. The negative δ^{56}Fe value for the surface soil suggests one of the following: (1) Fe loss has occurred without fractionation; (2) the surface soil parent material has an anomalously low Fe/Nb ratio; or (3) some mechanism retains isotopically light Fe in the surface horizons relative to the subsurface horizons. Explanation 1 could be valid if proton-promoted dissolution of Fe dominates in the surface soils. In contrast with reductive and ligand-promoted dissolution of Fe, which both favor enrichment of heavy Fe in the solid phase (Beard and Johnson, 2004; Brantley et al., 2004) (Wiederhold et al., 2006), proton-promoted dissolution has been shown to *not* fractionate Fe (Skulan et al., 2002). However, it is unlikely that proton-promoted dissolution dominates in these organic-rich soils with documented Eh values corresponding to Fe reducing conditions (Fig. 1). Loss of colloidal Fe, although possibly significant on a mass basis, can be neglected because colloids from these soils also contain appreciable quantities of Nb (Thompson et al., 2006a) and thus would not constitute an "Fe loss" when normalized to Nb. Therefore, Explanation 1 is unlikely.

Explanation 2 could be explained by a surface soil that has been augmented with tephra from more recent alkalic eruptions of Haleakala. Scribner et al. (2006) surveyed fresh parent material (PM) near each of the MCG sites and found four theolitic basalts with Fe/Nb mass ratios of 2860±130 (1SD) and one alkalic basalt with Fe/Nb mass ratio of ca. 1600 (A. Kurtz, personal communication). Recalculating τ_{Fe} using the alkalic PM yields a Rayleigh modeled PM δ^{56}Fe value of −0.17 (3)‰, very close to the accepted δ^{56}Fe value of Hawaiian basalts (δ^{56}Fe= −0.10(3)‰ Beard et al., 2003). Although Scribner et al. (2006) found mass balance data for multiple elements better fit a theolitic parent material, we cannot rule out the possibility that the MCG surface soils are augmented with alkalic material.

Internal cycling of Fe between aboveground vegetation and the surface soil organic matter may conserve isotopically light Fe in the surface horizons. Measurements of leaf fall collected at the 3500-mm MAP site indicate vegetation is lighter than the surface soil A horizon by ca. 0.1‰ (Table 2, Fig. 5); this is consistent with the findings of Walczyk and von Blanckenburg (2002) for the Fe isotopic composition of food plants. With foliar Fe concentrations for the dominant tree along the MCG (*M. polymorpha*; 75% of total biomass) ranging from 100 to 200 mg kg^{-1} (Schuur and Matson, 2001), Explanation 3 may be relevant if plant Fe cycling rates are rapid relative to the rate of Fe loss. Wiegand et al. (2005) found plant-induced cycling of Ca was responsible for isotopically light Ca in surface horizons of similar basaltic soils; the same may be true for Fe. However, without measurements of the Fe cycling rates between vegetation and surface horizons we cannot unequivocally evaluate the contribution of Explanation 2 or 3 to the isotopic composition of the surface horizons.

5. Conclusion

We have demonstrated that Rayleigh fractionation of Fe isotopes occurs during pedogenesis using a set of field sites well constrained to systematic variation in reductive dissolution along a climate gradient in Hawaii. δ^{56}Fe values increase with increasing removal of Fe from the soils consistent with Rayleigh fractionation yielding identical slopes (e.g., fractionation factors) for

the surface and subsurface horizons ($10^3 \ln\alpha_{lost-retained} \approx -0.36$). Our calculated fractionation factor is about a third the magnitude of experimentally determined values for reductive dissolution (Beard et al., 1999; Beard et al., 2003; Icopini et al., 2004), most likely reflecting Fe re-precipitation and organic complexation that modulate the net Fe loss in these organic rich, redox dynamic soils. The Rayleigh modeled intercepts ($\delta^{56}Fe_{initial}$) for the subsurface horizon are in agreement with the known isotopic composition of Hawaiian basalt. The $\delta^{56}Fe_{initial}$ for the surface horizons are ca. 0.3‰ less than known Hawaiian basalt composition indicating either (1) variation in parent material Fe/Nb ratios or (2) Fe isotopic depletion of the surface horizon, possibly due to internal Fe cycling between above-ground vegetation and the surface soil. In either case, this study validates experimental and theoretical predictions that reductive dissolution of Fe minerals results in a preferential loss of lighter Fe isotopes from open soil systems.

Acknowledgments

We thank Peter Vitousek for his leadership on the Hawaii Ecosystems Project and Heraldo Farrington for logistical and sampling assistance in the field. We also thank Mary Kay Amistadi for ICP-MS analysis, Mark Baker for his extensive assistance and operational expertise with the GVI *Isoprobe* and Ben Houlton for providing the leaf-fall samples. Gratitude is also expressed to Brian Beard for discussions regarding MC-ICP-MS analysis on the *Isoprobe*. This research was supported by National Research Initiative Competitive Grant no. 2003-35107-13663 from the USDA Cooperative State Research, Education, and Extension Service, and National Science Foundation Grant no. DEB-0212245. Finally, we thank S.M. Kraemer and one anonymous reviewer for helpful comments that greatly improved this manuscript.

References

Albarede, F., Beard, B., 2004. Analytical methods for non-traditional isotopes. Rev. Mineral. Geochem. 55, 113–152.

Anbar, A.D., Jarzecki, A.A., Spiro, T.G., 2005. Theoretical investigation of iron isotope fractionation between $Fe(H_2O)_6^{3+}$ and $Fe(H_2O)_6^{2+}$: implications for iron stable isotope geochemistry. Geochim. Cosmochim. Acta 69, 825–837.

Arnold, G.L., Weyer, S., Anbar, A.D., 2004. Fe isotope variations in natural materials measured using high mass resolution multiple collector ICPMS. Anal. Chem. 76, 322–327.

Balci, N., Bullen, T.D., Witte-Lien, K., Shanks, W.C., Motelica, M., Mandernack, K.W., 2006. Iron isotope fractionation during microbially stimulated Fe(II) oxidation and Fe(III) precipitation. Geochim. Cosmochim. Acta 70, 622–639.

Bartlett, R.J., James, B.R., 1993. Redox chemistry of soils. Adv. Agron. 151–208.

Beard, B.L., Johnson, C.M., 2004. Fe isotope variations in the modern and ancient earth and other planetary bodies. Rev. Mineral. Geochem. 55, 319–357.

Beard, B.L., Johnson, C.M., Cox, L., Sun, H., Nealson, K.H., Aguilar, C., 1999. Iron isotope biosignatures. Science 285, 1889–1892.

Beard, B.L., Johnson, C.M., Skulan, J.L., Nealson, K.H., Cox, L., Sun, H., 2003. Application of Fe isotopes to tracing the geochemical and biological cycling of Fe. Chem. Geol. 195, 87–117.

Brantley, S.L., Liermann, L., Bullen, T.D., 2001. Fractionation of Fe isotopes by soil microbes and organic acids. Geology 29, 535–538.

Brantley, S.L., Liermann, L.J., Guynn, R.L., Anbar, A., Icopini, G.A., Barling, J., 2004. Fe isotopic fractionation during mineral dissolution with and without bacteria. Geochim. Cosmochim. Acta 68, 3189–3204.

Bullen, T.D., White, A.F., Childs, C.W., Vivit, D.V., Schulz, M.S., 2001. Demonstration of significant abiotic iron isotope fractionation in nature. Geology 29, 699–702.

Casey, W.H., Banfield, J.F., Westrich, H.R., McLaughlin, L., 1993. What do dissolution experiments tell us about natural weathering? Chem. Geol. 105, 1–15.

Chadwick, O.A., Chorover, J., 2001. The chemistry of pedogenic thresholds. Geoderma 100, 321–353.

Chadwick, O.A., Brimhall, G.H., Hendricks, D.M., 1990. From a black to a gray box: a mass balance interpretation of pedogenesis. Geomorphology 3, 369–390.

Chadwick, O.A., Gavenda, R.T., Kelly, E.F., Ziegler, K., Olson, C.G., Elliott, W.C., et al., 2003. The impact of climate on the biogeochemical functioning of volcanic soils. Chem. Geol. 202, 195–223.

Chorover, J., Amistadi, M.K., Chadwick, O.A., 2004. Surface charge evolution of mineral-organic complexes during pedogenesis in Hawaiian basalt. Geochim. Cosmochim. Acta 68, 4859–4876.

Cornell, R.M., Schwertmann, U., 1996. The iron oxides: structure, properties, reactions, occurrence and uses. The Iron Oxides. VCH, New York, NY.

Crews, T.E., Kitayama, K., Fownes, J.H., Riley, R.H., Herbert, D.A., Muellerdombois, D., et al., 1995. Changes in soil-phosphorus fractions and ecosystem dynamics across a long chronosequence in Hawaii. Ecology 76, 1407–1424.

Crosby, H.A., Johnson, C.M., Roden, E.E., Beard, B.L., 2005. Coupled Fe(II)-Fe(III) electron and atom exchange as a mechanism for Fe isotope fractionation during dissimilatory iron oxide reduction. Environ. Sci. Technol. 39, 6698–6704.

Darke, A.K., Walbridge, M.R., 2000. Al and Fe biogeochemistry in a floodplain forest: implications for P retention. Biogeochemistry 51, 1–32.

Emmanuel, S., Erel, Y., Matthews, A., Teutsch, N., 2005. A preliminary mixing model for Fe isotopes in soils. Chem. Geol. 222, 23–34.

Fantle, M.S., DePaolo, D.J., 2004. Iron isotopic fractionation during continental weathering. Earth Planet. Sci. Lett. 228, 547–562.

Hinsinger, P., Barros, O.N.F., Benedetti, M.F., Noack, Y., Callot, G., 2001. Plant-induced weathering of a basaltic rock: experimental evidence. Geochim. Cosmochim. Acta 65, 137–152.

Hossner, L.R., 1996. Dissolution for total elemental analysis. In: Sparks, D.L. (Ed.), Methods of Soil Analysis: Part 3—Chemical Methods. Soil Science Society of America, Madison, WI, pp. 49–64.

Icopini, G.A., Anbar, A.D., Ruebush, S.S., Tien, M., Brantley, S.L., 2004. Iron isotope fractionation during microbial reduction of iron: the importance of adsorption. Geology 32, 205–208.

Ingri, J., Malinovsky, D., Rodushkin, I., Baxter, D.C., Widerlund, A., Andersson, P., et al., 2006. Iron isotope fractionation in river colloidal matter. Earth Planet. Sci. Lett. 245, 792–798.

Jansen, B., Nierop, K.G.J., Verstraten, J.M., 2003. Mobility of Fe(II), Fe(III) and al in acidic forest soils mediated by dissolved organic matter: influence of solution pH and metal/organic carbon ratios. Geoderma 113, 323–340.

Jenny, H., 1941. Factors of Soil Formation. Academic Press, New York.

Jeon, B.-H., Dempsey, B.A., Burgos, W.D., Royer, R.A., 2001. Reactions of ferrous iron with hematite. Colloid Surf. A 191, 41–55.

Johnson, C.M., Beard, B.L., Roden, E.E., Newman, D.K., Nealson, K.H., 2004. Isotopic constraints on biogeochemical cycling of Fe. Rev. Mineral. Geochem. 55, 359–408.

Kurtz, A.C., Derry, L.A., Chadwick, O.A., Alfano, M.J., 2000. Refractory element mobility in volcanic soils. Geology 28, 683–686.

Küsel, K., Wagner, C., Trinkwalter, T., Göβner, A.S., Baumler, R., Drake, H.L., 2002. Microbial reduction of Fe(III) and turnover of acetate in Hawaiian soils. FEMS Microbiol. Ecol. 40, 73–81.

Loeppert, R.H., Inskeep, W.P., 1996. Iron. In: Sparks, D.L. (Ed.), Methods of Soil Analysis: Part 3—Chemical Methods. Soil Science Society of America, pp. 639–664.

Lovley, D.R., Phillips, E.J.P., 1986. Organic-matter mineralization with reduction of ferric iron in anaerobic sediments. Appl. Environ. Microbiol. 51, 683–689.

Matthews, A., Zhu, X.-K., O'Nions, K., 2001. Kinetic iron stable isotope fractionation between iron (-II) and (-III) complexes in solution. Earth Planet. Sci. Lett. 192, 81–92.

Miller, A.J., Schuur, E.A.G., Chadwick, O.A., 2001. Redox control of phosphorus pools in Hawaiian montane forest soils. Geoderma 102, 219–237.

Mullane, E., Russell, S.S., Gounelle, M., Mason, T., Din, V., Weiss, D., et al., 2002. Precise and accurate determination of iron isotopes by multicollector inductively coupled plasma mass spectrometry. In: Holland, G., Tanner, S.D. (Eds.), Plasma Source Mass Spectrometry: Applications and Emerging Technologies. The Royal Society of Chemistry, Cambridge, UK, pp. 351–361.

Parfitt, R.L., Childs, C.W., Eden, D.N., 1988. Ferrihydrite and allophane in four andepts from Hawaii and implications for their classification. Geoderma 41, 223–241.

Ponnamperuma, F., 1972. The chemistry of submerged soils. Adv. Agron. 24, 29–96.

Schuur, E.A.G., Matson, P.A., 2001. Net primary productivity and nutrient cycling across a mesic to wet precipitation gradient in Hawaiian montane forest. Oecologia 128, 431–442.

Schwertmann, U., 1991. Solubility and dissolution of iron-oxides. Plant Soil 130, 1–25.

Scribner, A.M., Kurtz, A.C., Chadwick, O.A., 2006. Germanium sequestration by soil: targeting the roles of secondary clays and Fe-oxyhydroxides. Earth Planet. Sci. Lett. 243, 760–770.

Severmann, S., Johnson, C.M., Beard, B.L., McManus, J., 2006. The effect of early diagenesis on the Fe isotope compositions of porewaters and authigenic minerals in continental margin sediments. Geochim. Cosmochim. Acta 70, 2006–2022.

Shoji, S., Nanzyo, M., Dahlgren, R.A., 1993. Volcanic ash soils: genesis, properties and utilization. Dev. Soil Sci., vol. 21. Elsevier, New York.

Skoog, D.A., West, D.M., Holler, F.J., 1997. Fundamentals of Analytical Chemistry. Saunders College Publishing, Orlando, FL. (870 pp.).

Skulan, J., Beard, B., Johnson, C., 2002. Kinetic and equilibrium Fe isotope fractionation between aqueous Fe(III) and hematite. Geochim. Cosmochim. Acta 66, 2995–3015.

Stewart, B.W., Capo, R.C., Chadwick, O.A., 2001. Effects of rainfall on weathering rate, base cation provenance, and sr isotope composition of Hawaiian soils. Geochim. Cosmochim. Acta 65, 1087–1099.

Taylor, P.D.P., Maeck, R., Debievre, P., 1992. Determination of the absolute isotopic composition and atomic-weight of a reference sample of natural iron. Int. J. Mass Spectrom. Ion Processes 121, 111–125.

Thompson, A., Chadwick, O.A., Boman, S., Chorover, J., 2006a. Colloid mobilization during soil iron redox oscillations. Environ. Sci. Technol. 40, 5743–5749.

Thompson, A., Chadwick, O.A., Rancourt, D.G., Chorover, J., 2006b. Iron-oxide crystallinity increases during soil redox oscillations. Geochim. Cosmochim. Acta 70, 1710–1727.

Torn, M.S., Trumbore, S.E., Chadwick, O.A., Vitousek, P.M., Hendricks, D.M., 1997. Mineral control of soil organic carbon storage and turnover. Nature 389, 170–173.

Vitousek, P.M., 2004. Nutrient Cycling and Limitation: Hawaii as a Model System. Princeton University Press, Princeton. (232 pp.).

Wada, K., Wada, S.-I., 1976. Clay mineralogy of the b horizons of two hydrandepts, a torrox and a humitropept in Hawaii. Geoderma 16, 139–157.

Walczyk, T., von Blanckenburg, F., 2002. Natural iron isotope variations in human blood. Science 295, 2065–2066.

White, A.F., Brantley, S.L., 2003. The effect of time on the weathering of silicate minerals: why do weathering rates differ in the laboratory and field? Chem. Geol. 202, 479–506.

Wiederhold, J.G., Kraemer, S.M., Teutsch, N., Borer, P.M., Halliday, A.N., Kretzschmar, R., 2006. Iron isotope fractionation during proton-promoted, ligand-controlled, and reductive dissolution of goethite. Environ. Sci. Technol. 40, 3787–3793.

Wiegand, B.A., Chadwick, O.A., Vitousek, P.M., Wooden, J.L., 2005. Ca cycling and isotopic fluxes in forested ecosystems in Hawaii. Geophys. Res. Lett. 32 (Art. no. L11404).